Modelling of Sympathetic String Vibrations

Jean-Loic Le Carrou, François Gautier, Nicolas Dauchez, Joël Gilbert

Modelling of Sympathetic String Vibrations

Jean-Loïc Le Carrou,* Francois Gautier, Nicolas Dauchez, and Joël Gilbert
Laboratoire d'Acoustique de l'Université du Maine,
UMR CNRS 6613, 72085 Le Mans Cedex 9, France
(Dated: October 5, 2004)

Abstract

String instruments are usually composed of several strings connected to a vibrating body allowing efficient sound radiation. For some special string tunings, sympathetic vibrations can occur: if one string is excited, some others are also excited via the body.

In order to investigate this phenomenon, an analytical model of a simplified generic string instrument has been developed. The body of the instrument is represented by a beam clamped at both ends, to which several strings are attached. The state vector formalism and the transfer matrix method are used to describe the propagation of bending and extensional waves in each sub-structure (strings and beam). Coupling conditions between sub-structures take into account the angle formed by the beam and the strings. This leads to a linear system from which the normal modes of the assembly are computed. Numerical computations are carried out in the case of the beam-2 strings assembly and mode shapes are classified thanks to a criterion, the kinetic energy ratio (KER). Four kinds of modes may be identified: beam modes, string modes, beam-string modes and string-string modes. The latter are responsible for sympathetic response. An experimental modal analysis carried out on a clamped beam equiped with two strings confirms our theoretical results.

PACS numbers: 43.40.Cw, 43.75.Gh

*Electronic address: jean-loic.le_carrou@univ-lemans.fr

I. INTRODUCTION

String instruments are usually composed of several strings connected to a vibrating body allowing efficient sound radiation. The plane part of this vibrating body is called soundboard and is generally a stiffened and tapered plate of complex shape, made from different materials. When no dampers are applied to the strings, important coupling between them can occur via the soundboard: if one string is excited, other strings can vibrate and contribute significantly to the musical sound. This phenomenon is known as *sympathetic vibration* and is defined in the dictionary of acoustics [1] as "resonant or near-resonant response of a mechanical or acoustical system excited by energy from an adjoining system in steady-state vibration".

For some instruments such as the viola d'amore, the baryton or non-european instruments like the sitar or the sarangi, sympathetic string vibrations result in a characteristic sound quality: these instruments have additional strings designed to be sympathetically excited by the main strings [2]. In the case of the violin, sympathetic vibration is highlighted in [3]: "if one plays the D on the violin G string which matches the pitch of the open D string and alternately damps and undamps the open D with a finger, the reading on the meter can be observed to increase about 1-2 dB as the open string is damped. The effect is more noticeable on a cello or bass".

Numerous strings of the piano are organised in pairs or triplets (bichord or trichord) in which the strings are almost tuned in unison. The coupling of these strings has been investigated in [4, 5, 6]: a model for the normal modes of strings pairs has been developed taking into account mistuning from unison and the finite admittance of the bridge at the connection point of the strings. The role of string's polarization is also pointed out: resistive and reactive parts of the admittance may differ for 'horizontal' and 'vertical' vibration. With this 'anisotropic boundary conditions', interactions in the time domain between normal modes lead to beats and double decay rates in the aftersound. Since the hammer excites simultaneously the group of two (or three) strings, the tone does not involve as such a sympathetic vibration. This sympathetic vibration exists when the una corda pedal is used. In this case, the hammer is mechanically shifted and only one string out of two (or two out of three) is struck. Coupling between the initially excited string and the other string leads then to sympathetic vibration [5].

Note that the sympathetic vibration effect has been included in time domain simulation of piano tones to get realistic synthesis sound. For such simulations, a phenomenological model of the coupling between strings is introduced and no physical model of the coupling are described [7].

The harp is the main instrument to which this study can be applied. For this instrument, the sympathetic vibration effect appears as soon as a string is excited because all the strings are undamped. This effect remains even if the excited string is damped. Although this effect is a fundamental characteristic of the instrument, the instrument maker has to design the

harp in such a manner that sympathetic vibration remains reasonable. Note that the case of the harp has some particularities: each string is tuned differently from the others and no pair of strings exists. Different strings can interact even if they are connected to remote points of the soundboard. In this case, the local admittance of the soundboard is not a sufficient parameter and structure-borne sound inside the soundboard has to be taken into account. The whole soundboard and the strings have to be studied as a coupled system.

The aim of this paper is to present a modelling of sympathetic vibration on a simplified string instrument. The main application is related to the case of the harp but the formulation can be adapted to the piano's configuration. This model allows us to determine the normal modes of a structure coupled to a great number of strings and to identify those which are responsible for the sympathetic phenomenon.

The paper is structured as follows: first, the state vector formalism and the transfer matrix method are presented and applied to obtain the normal modes of a beam-N strings assembly. The case of a beam-2 strings assembly is then highlighted. Numerical results for modes shapes of the assembly are given and classification of these modes is proposed using an appropriated criterion. Experimental modal analysis is also performed on the studied beam-2 strings assembly and confirms the theoretical results. Finally, the influence of inharmonicity on the modes, responsible for sympathetic vibration, is studied.

II. MODEL OF A BEAM-N STRINGS ASSEMBLY

In order to investigate couplings between strings via the instrument's soundboard, we consider a simplified configuration: the soundboard is represented by a simple beam, on which several strings are connected. Such a choice allows to describe the structure-borne coupling in an analytical way. The aim of this section is to present a method for calculating modes of a beam-N string assembly: the state vector formalism and the transfer matrix method are applied in this context in order to obtain the normal modes (eigenfrequencies and mode shapes) of the assembly.

A. Description of the assembly

The beam-N strings assembly is described in figure 1. This plane assembly is constituted of a uniform, prismatic beam on which N different strings are connected. The beam is supposed to be clamped at points A and B. The extremity O_i of the i-string (i=1...N) is the string connection point to the beam. The other extremity C_i of the i-string is supposed to be simply supported. The angle α_i between the axis (A, x_b) of the beam and the axis (A, x_{si}) of the i-string induces coupling between longitudinal and bending vibrations in the beam and in the i-string. In the case of the harp, this angle is about 40°.

The chosen configuration is well adapted to the case of the harp: for this instrument, the

strings are connected on the symmetry line of the soundboard, and thus its vibrations can be modelled using an equivalent beam.

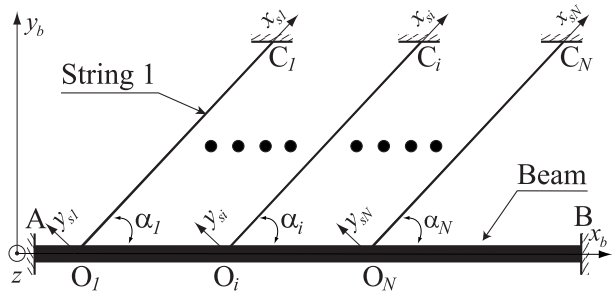

FIG. 1: Diagram of a clamped-clamped beam connected to several fixed strings. It includes local coordinate sytems and the notation used.

B. Transfer Matrix for a uniform sub-structure

In harmonic regime (e^{jwt}), the vibratory state of each sub-structure (string or beam) of the assembly is described at any point of its neutral line by a state vector denoted by $\boldsymbol{\mathcal{X}}(x)$ whose components are kinematic and force variables [8, 9, 10]. The same generic name x is used to denote the space coordinate in the beam and in the strings. It permits us to present in the same manner the motion equations related to beam and to strings. In figure 1, the coordinate x correspond to x_b for the beam and to x_{si} for the i-string. For the i-string, the state vector is the 4-by-1 vector,

$$\boldsymbol{\mathcal{X}}_s(x) = \begin{pmatrix} u_s(x) \\ w_s(x) \\ N_s(x) \\ Q_s(x) \end{pmatrix}, \tag{1}$$

where u_s, w_s are the longitudinal and transversal displacements and N_s, Q_s are the longitudinal and transversal forces. In the beam, the state vector is the 6-by-1 vector:

$$\boldsymbol{\mathcal{X}}_b(x) = \begin{pmatrix} u_b(x) \\ w_b(x) \\ \theta_b(x) \\ N_b(x) \\ Q_b(x) \\ M_b(x) \end{pmatrix}, \tag{2}$$

where $u_b(x)$, $w_b(x)$ and θ_b are respectively the longitudinal, transverse displacements and the slope of the beam cross section (figure 2) and where $N_b(x)$, $Q_b(x)$ and $M_b(x)$ are re-

spectively the longitudinal transverse forces and bending moment. Note that longitudinal displacements are taken into account to ensure kinematic continuities.

The beam and strings bending motions are respectively described in the framework of the elastic string's theory [11] and of the Euler-Bernoulli beam model [12]. Extensionnal motions are described in the framework of classical rod theory [12]. No dissipative phenomena are included. For all these kinematic models, the equations of motion of a sub-structure (beam or string) can be written as a first order differential matrix equation, called state equation,

$$\frac{d\boldsymbol{\mathcal{X}}(x)}{dx} = \mathrm{H}(\omega)\boldsymbol{\mathcal{X}}(x). \tag{3}$$

Matrix $\mathrm{H}(\omega)$ is the characteristic matrix of the sub-structure. Since each sub-structure is supposed to be uniform, the matrix $\mathrm{H}(\omega)$ is a space invariant matrix depending only on the angular frequency ω. The solution of (3) can be written [8, 9] as

$$\boldsymbol{\mathcal{X}}(x) = \mathrm{T}(x, x_0)\boldsymbol{\mathcal{X}}(x_0), \tag{4}$$

where $\mathrm{T}(x, x_0)$ is the transfer matrix between the state vector at point x_0 and the state vector at point x. This transfer matrix can be straightforwardly determined from matrix H. It is given by

$$\mathrm{T}(x, x_0) = \mathrm{E}Q(x, x_0)\mathrm{E}^{-1}, \tag{5}$$

where E is the matrix of eigenvectors of matrix N, defined by $\mathrm{H} = \jmath\mathrm{N}$. Matrix E obeys the fundamental relationship,

$$\mathrm{NE} = \mathrm{E}\Lambda, \tag{6}$$

where Λ is the diagonal matrix whose terms are the eigenvalues $((\lambda_k)_{k=1\ldots N})$ of the matrix N,

$$\Lambda = diag(\lambda_k). \tag{7}$$

Each eigenvalue λ_k corresponds to a wavenumber. Since the beam and the strings have an axial symmetry, these eigenvalues appear by pairs $(\lambda_k, -\lambda_k)$ corresponding to wave propagation in two opposite directions. In relation (5), the matrix $Q(x, x_0)$ is the propagator matrix given by

$$Q(x, x_0) = diag\left(e^{\jmath\lambda_k(x-x_0)}\right). \tag{8}$$

For beam and string's segments, the expression of the characteristic matrix $\mathrm{H}(\omega)$ and the transfer matrix $\mathrm{T}(x, x_0)$ are given in appendices A and B.

C. Coupling equations at beam-string connection point

The connection between the beam and the i-string is shown in figure 2. Points O_i^- and O_i^+ are limit points of the connection volume belonging to the beam's parts. Point O_i is the limit point belonging to the i-string.

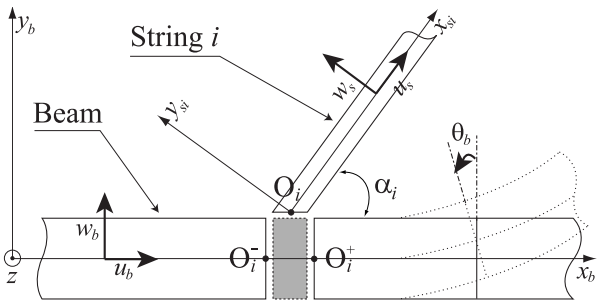

FIG. 2: Connection between beam and string including local coordinate sytem and notations. In grey, the connection volume, supposed to be very small.

Since the connection volume is supposed to be very small, kinematic continuity relations are assumed:

$$u_b(O_i^-) = u_b(O_i^+) \tag{9}$$
$$w_b(O_i^-) = w_b(O_i^+) \tag{10}$$
$$\theta_b(O_i^-) = \theta_b(O_i^+) \tag{11}$$
$$u_s(O_i) = u_s(O_i^+)\cos(\alpha_i) + w_s(O_i^+)\sin(\alpha_i) \tag{12}$$
$$w_s(O_i) = -u_s(O_i^+)\sin(\alpha_i) + w_s(O_i^+)\cos(\alpha_i). \tag{13}$$

Mass and rotational inertia of the connection volume are ignored, it implies that the sum of the force and of the moment continuity applied to the connection equal zero. Projecting such relations on the local axis (x_b, y_b, z) leads to

$$N_b(O_i^+) - N_b(O_i^-) + N_s(O_i)\cos(\alpha_i) - Q_s(O_i)\sin(\alpha_i) = 0 \tag{14}$$
$$Q_b(O_i^+) - Q_b(O_i^-) + N_s(O_i)\sin(\alpha_i) + Q_s(O_i)\cos(\alpha_i) = 0 \tag{15}$$
$$M_b(O_i^+) - M_b(O_i^-) = 0. \tag{16}$$

Using the state vector formalism introduced in (1) and (2), coupling equations (9) to (16) can be written on matrix forms as:

$$\boldsymbol{\mathcal{X}_b}(O_i^+) = \boldsymbol{\mathcal{X}_b}(O_i^-) + \mathrm{K}_i\boldsymbol{\mathcal{X}_s}(O_i) \tag{17}$$

and

$$L\boldsymbol{\mathcal{X}_s}(O_i) + M_i\boldsymbol{\mathcal{X}_b}(O_i^+) = 0, \tag{18}$$

where

$$L = \begin{pmatrix} 1 & 0 & 0 & 0 \\ 0 & 1 & 0 & 0 \end{pmatrix}, M_i = \begin{pmatrix} \cos(\alpha_i) & \sin(\alpha_i) & 0 & 0 & 0 & 0 \\ -\sin(\alpha_i) & \cos(\alpha_i) & 0 & 0 & 0 & 0 \end{pmatrix}.$$

and

$$\mathrm{K}_i = \begin{pmatrix} 0 & 0 & 0 & 0 \\ 0 & 0 & 0 & 0 \\ 0 & 0 & 0 & 0 \\ 0 & 0 & -\cos(\alpha_i) & \sin(\alpha_i) \\ 0 & 0 & -\sin(\alpha_i) & -\cos(\alpha_i) \\ 0 & 0 & 0 & 0 \end{pmatrix}.$$

The matrices L and M_i are called continuity matrices. The matrix K_i is a coupling matrix, depending on the connection angle α_i, which is responsible for the coupling between longitudinal and transverse motions in each string and in the beam.

D. Modes of the assembly

The state vector at one point of the assembly depends on the state vector on its boundary points: A, B, C_1, ..., C_N. For these particular points, the number of state vector components is 12+4N: 12 for the beam state vectors ($\boldsymbol{\mathcal{X}}_{\boldsymbol{b}}(A)$ and $\boldsymbol{\mathcal{X}}_{\boldsymbol{b}}(B)$) and 4$N$ for the N string state vectors ($\boldsymbol{\mathcal{X}}_{\boldsymbol{s}}(C_1)$, ..., $\boldsymbol{\mathcal{X}}_{\boldsymbol{s}}(C_i)$). Half of these 12+4$N$ state vector components are imposed by boundary conditions. In the case of the clamped beam and of the fixed strings ends that are considered here, every kinematic variables, indicated by index k (displacements and slopes), are set to zero. Forces variables, indicated by index f (forces and moments) are unknown and do not equal zero. Equations of the assembly impose 6+2N transfer relations between the 6+2N components of the boundary state vectors.

A first set of 2N equations is given by the following relation, proved in appendix C, for $i = 1...N$,

$$L\mathrm{T}_s(O_i, C_i)\boldsymbol{\mathcal{X}}_{\boldsymbol{s}}(C_i) + \mathrm{M}_i\mathrm{T}_b(O_i^+, A)\boldsymbol{\mathcal{X}}_{\boldsymbol{b}}(A) + \sum_{j=1}^{i}\left[\mathrm{M}_i\mathrm{T}_b(O_i^-, O_j^+)\mathrm{K}_j\mathrm{T}_s(O_j, C_j)\boldsymbol{\mathcal{X}}_{\boldsymbol{s}}(C_j)\right] = 0. \tag{19}$$

A second set of 6 equations is obtained when the transfer relation between state vectors $\boldsymbol{\mathcal{X}}_{\boldsymbol{b}}(O_N^+)$ and $\boldsymbol{\mathcal{X}}_{\boldsymbol{b}}(B)$, given by

$$\boldsymbol{\mathcal{X}}_{\boldsymbol{b}}(O_N^+) = \mathrm{T}(x_{O_N}, x_B)\boldsymbol{\mathcal{X}}_{\boldsymbol{b}}(B), \tag{20}$$

is associated to the recurrence relation (C1), leading to:

$$\boldsymbol{\mathcal{X}}_{\boldsymbol{b}}(A) - \mathrm{T}_b(A, B)\boldsymbol{\mathcal{X}}_{\boldsymbol{b}}(B) + \sum_{j=1}^{N}\left[\mathrm{T}_b(A, O_j^+)\mathrm{K}_j\mathrm{T}_s(O_j, C_j)\boldsymbol{\mathcal{X}}_{\boldsymbol{s}}(C_j)\right] = 0. \tag{21}$$

The set of 6+2N independent scalar relations given above may be written in matrix form

as:

$$R \begin{pmatrix} \boldsymbol{\mathcal{X}_b}(A) \\ \boldsymbol{\mathcal{X}_b}(B) \\ \boldsymbol{\mathcal{X}_s}(C_1) \\ \vdots \\ \boldsymbol{\mathcal{X}_s}(C_N) \end{pmatrix} = \left(\begin{array}{c|c} R_1 & R_2 \\ \hline R_3 & R_4 \end{array}\right) \begin{pmatrix} \boldsymbol{\mathcal{X}_b}(A) \\ \boldsymbol{\mathcal{X}_b}(B) \\ \boldsymbol{\mathcal{X}_s}(C_1) \\ \vdots \\ \boldsymbol{\mathcal{X}_s}(C_N) \end{pmatrix} = \begin{pmatrix} 0 \\ \vdots \\ \vdots \\ \vdots \\ 0 \end{pmatrix} \tag{22}$$

where

$$R_1 = \begin{pmatrix} I_6 & -\mathrm{T}_b(A,B) \end{pmatrix}, \tag{23}$$

$$R_2 = \begin{pmatrix} \mathrm{T}_b(A,O_1^+)\mathrm{K}_1\mathrm{T}_s(O_1,C_1) & \cdots & \mathrm{T}_b(A,O_N^+)\mathrm{K}_N\mathrm{T}_s(O_N,C_N) \end{pmatrix}, \tag{24}$$

$$R_3 = \begin{pmatrix} \mathrm{M}_1\mathrm{T}_b(O_1^+,A) & 0 \\ \vdots & \vdots \\ \mathrm{M}_N\mathrm{T}_b(O_N^+,A) & 0 \end{pmatrix}, \tag{25}$$

$$R_4 = \begin{pmatrix} L\mathrm{T}_s(O_1,C_1) & 0 & \cdots & 0 \\ \mathrm{M}_2\mathrm{T}_b(O_2^-,O_1^+)K_1\mathrm{T}_s(O_1,C_1) & L\mathrm{T}_s(O_2,C_2) & \cdots & \vdots \\ & \vdots & & 0 \\ \mathrm{M}_N\mathrm{T}_b(O_N^-,O_1^+)K_1\mathrm{T}_s(O_1,C_1) & \cdots & \mathrm{M}_N\mathrm{T}_b(O_N^-,O_{N-1}^+)K_{N-1}\mathrm{T}_s(O_{N-1},C_{N-1}) & \mathrm{LT}_s(O_N,C_N) \end{pmatrix} \tag{26}$$

Thus, the 12+4N-by-1 vector of state vectors at the ends, explicited in the relation (22), can be written on the following form taken into account the components set to zero because of boundary conditions:

$$\begin{pmatrix} \boldsymbol{\mathcal{X}_b}(A) \\ \boldsymbol{\mathcal{X}_b}(B) \\ \boldsymbol{\mathcal{X}_s}(C_1) \\ \vdots \\ \boldsymbol{\mathcal{X}_s}(C_N) \end{pmatrix} = \begin{pmatrix} \boldsymbol{\mathcal{X}_b^k}(A) \\ \boldsymbol{\mathcal{X}_b^f}(A) \\ \boldsymbol{\mathcal{X}_b^k}(B) \\ \boldsymbol{\mathcal{X}_b^f}(B) \\ \boldsymbol{\mathcal{X}_s^k}(C_1) \\ \boldsymbol{\mathcal{X}_s^f}(C_1) \\ \vdots \\ \boldsymbol{\mathcal{X}_s^k}(C_N) \\ \boldsymbol{\mathcal{X}_s^f}(C_N) \end{pmatrix} = \begin{pmatrix} 0 \\ \boldsymbol{\mathcal{X}_b^f}(A) \\ 0 \\ \boldsymbol{\mathcal{X}_b^f}(B) \\ 0 \\ \boldsymbol{\mathcal{X}_s^f}(C_1) \\ \vdots \\ 0 \\ \boldsymbol{\mathcal{X}_s^f}(C_N) \end{pmatrix} = \begin{pmatrix} 0_3 & \cdots & \cdots & \cdots & 0_3 \\ I_3 & \cdots & \cdots & \cdots & \vdots \\ 0_3 & 0_3 & \cdots & \cdots & \vdots \\ 0_3 & I_3 & 0_3 & \cdots & \vdots \\ \vdots & 0_2 & 0_2 & \cdots & \vdots \\ \vdots & \vdots & I_2 & 0_2 & \vdots \\ \vdots & \vdots & 0_2 & \ddots & \vdots \\ \vdots & \vdots & \vdots & \vdots & 0_2 \\ 0_2 & \cdots & \cdots & 0_2 & I_2 \end{pmatrix} \begin{pmatrix} \boldsymbol{\mathcal{X}_b^f}(A) \\ \boldsymbol{\mathcal{X}_b^f}(B) \\ \boldsymbol{\mathcal{X}_s^f}(C_1) \\ \vdots \\ \boldsymbol{\mathcal{X}_s^f}(C_N) \end{pmatrix} = Z\boldsymbol{\mathcal{X}^f}, \tag{27}$$

where $\boldsymbol{\mathcal{X}^f}$ denotes the force variables of all state vectors at the boundaries. Therefore, 6+2N relations remain along with the 6+2N unknown variables of state vectors and may be written as

$$(R \cdot Z)\,\boldsymbol{\mathcal{X}^f} = R_R\boldsymbol{\mathcal{X}^f} = 0. \tag{28}$$

In the case of free vibrations, vector $\boldsymbol{\mathcal{X}^f}$ is not equal to zero and the matrix R_R is not an inversible matrix, implying:

$$\det\left(\mathrm{R_R}(\omega)\right) = 0. \tag{29}$$

The angular eigenfrequencies ω_i of the system are obtained from equation (29). For each ω_i, relation (28) provides the components of $\boldsymbol{\mathcal{X}^f}$ (with an unknown multiplicative factor) from which we can perform all state vector components at any point on the assembly by equations (C1) and (20) and thus obtain the associated mode shape.

III. THE BEAM-2 STRINGS ASSEMBLY CASE

Using the beam-N strings model presented in section II, a numerical application is carried out in the case of the beam-2 strings assembly and validated by an experimental modal analysis.

A. Description

The structure used in experimental and theoretical studies is presented in figure 3. It is composed of 2 strings tuned on octave (the frequency of one almost equals the double of the other one's) at $\mathrm{E_2}$=82.4 Hz and $\mathrm{E_3}$=164.8 Hz on the equal temperament scale based on $\mathrm{A_4}$=440 Hz. Note that such values correspond to fundamental frequencies of uncoupled strings, allowing to determine the string's tension if we assume that the beam behaves like a fixed end. In order to avoid static deformation during the experiment, we choose to fix the strings not only on either side of the beam but also close to each other, figure 3. The strings and beam characteristics used in the numerical applications are presented in table I.

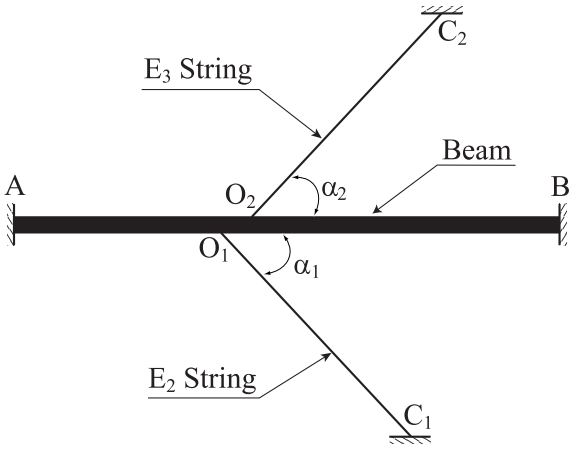

FIG. 3: Diagram of beam-2 strings tuned on octave.

	E_2 string	**E_3 string**	**Beam**
Length	L_s = 0.57 m		L_b = 1.315 m
Young Modulus	E_s = 210 GPa		E_b = 71 GPa
Section	A_1 = 1.41 mm^2	A_2 = 0.45 mm^2	A_b = 20×8 mm^2
Mass per unit length	ρ_1 = 11 10^{-3} kg/m	ρ_2 = 3.7 10^{-3} kg/m	ρ_b = 0.416 kg/m
Frequency	f_1 = 82.4 Hz	f_2 = 164.8 Hz	
Angle	α_1 = -43°	α_2 = 43°	
Connection points	A O_1 = 0.54 m	A O_2 = 0.58 m	

TABLE I: Parameters values of the beam-2 strings assembly.

B. Numerical results

1. Eigenfrequencies

Eigenfrequencies of the structure are computed from equation (29). The logarithm of matrix R_R determinant is shown in figure 4 as a function of frequency. Eigenfrequencies are given by each drop of the curve. We thus obtain 14 eigenfrequencies in the frequency range 0-500 Hz, shown in table II. For high frequencies, above 750 Hz, a numerical divergence occurs in the calculation of this determinant. As the frequency increases, the matrix R_R becomes ill-conditionned because of exponential terms with real argument present in the propagator matrix Q, defined by (8). This limitation of the transfer matrix method is well known and discussed, for example, in [8].

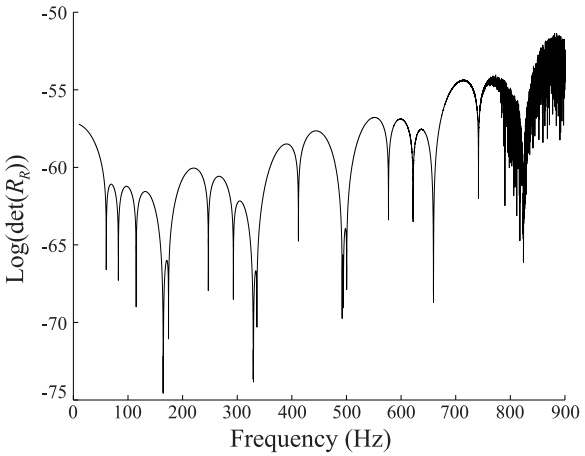

FIG. 4: Logarithm of the R_R matrix determinant as function of frequency. Each drop corresponds to an eigenfrequency.

2. Modes shapes and orthogonality check

For each eigenfrequency, we perform mode shapes of the structure. Table II shows the eigenfrequencies of modes and in figure 7-A are presented the corresponding mode shapes. Note that because of the transfer matrix method's frequency limitation, only transversal modes are obtained (the first longitudinal mode is about 2000 Hz for a clamped beam with the same characteristics as for the coupled one). To verify the validity of our calculation, we perform an orthogonality test of the modal basis using the dot product matrix of modes. This i-by-j Dot Product Matrix can be explicited for each term,

$$DPM(i,j) = \frac{< \mathbf{\Phi}_i, \mathbf{\Phi}_j >}{\sqrt{< \mathbf{\Phi}_i, \mathbf{\Phi}_i >}\sqrt{< \mathbf{\Phi}_j, \mathbf{\Phi}_j >}}, \tag{30}$$

where vector $\mathbf{\Phi}_i$ is the mode shape i,

$$\mathbf{\Phi}_i = \begin{pmatrix} u \\ w \end{pmatrix}_i \tag{31}$$

whose components are longitudinial and transversal displacements, and where the dot product is defined [12] by

$$< \mathbf{\Phi}_i, \mathbf{\Phi}_j >= \int_{\mathcal{S}} \rho_{\mathcal{S}} \; \mathbf{\Phi}_i^T(x) \; \mathbf{\Phi}_j(x) \; dx. \tag{32}$$

The dot product between modes i and j for a conservative structure ($\mathcal{S}$) equals one when $i = j$ and otherwise equals zero. This is illustrated in figure 5, which shows the orthogonality of modes.

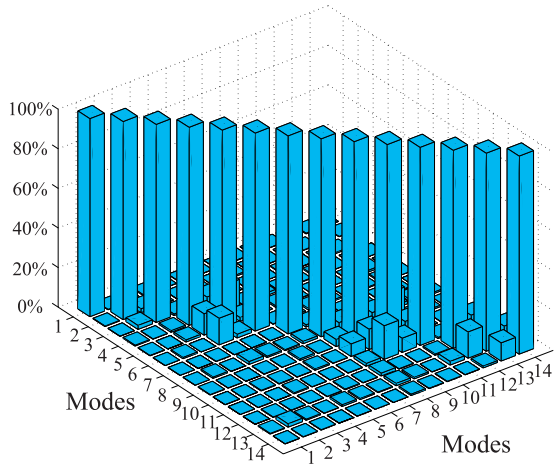

FIG. 5: Dot product matrix for the 14 first theoretical modes of the assembly.

Mode	Freq.	$KER_j(k)$			Kind	Uncoupled freq. (Hz)			
j	(Hz)	k=0	k=1	k=2	of mode	Beam*	E_2 String	E_3 String	Beam**
1	60.25	100	0	0	**Beam**	24.85			76.98
2	82.35	0	100	0	**String**		82.40		
3	114.95	100	0	0	**Beam**	68.50			141.18
4	164.45	6	25	69	**String-String**		164.80	164.80	
5	164.80	0	63	37	**String-String**				
6	174.20	99	0	1	**Beam**	134.30			212.72
7	247.10	0	100	0	**String**		247.20		
8	292.95	99	1	0	**Beam**	222.00			389.34
9	329.30	11	0	89	**Beam-String**	331.60	329.60	329.60	418.72
10	329.70	3	97	0	**String**				
11	335.95	97	0	3	**Beam**	331.60			418.72
12	412.00	2	98	0	**String**		412.00		
13	492.10	91	9	0	**Beam**	463.15			690.04
14	494.40	1	25	74	**String-String**		494.40	494.40	

TABLE II: Mode number, eigenfrequencies, kinetic energy ratio (k=0 for the Beam, k=1 for the E_2 string and k=2 for the E_3 string) and kinds of modes computed for the beam-2 strings assembly (left column). Eigenfrequencies of uncoupled sub-structures (beam*, E_2 string, E_3 string) with same characteristics as for coupled ones (middle column). Eigenfrequencies of beam constrained by nodes at the positions of string supports (denoted beam**), obtained by FEM (right column).

3. Definition of the criterion for modes classification

In order to classify modes of the assembly, we define an indicator, called kinetic energy ratio (KER), allowing us to determine in which sub-structure the modal shape displacement is the most important. Each sub-structure is indexed by k: k=0 for the beam, k=1 for the E_2 string and k=2 for the E_3 string. For each mode $\mathbf{\Phi}_j$, we define

$$KER_j(k) = \frac{\displaystyle\int_k \rho_k \ \omega_j^2 \ \mathbf{\Phi}_j^T(x)\mathbf{\Phi}_j(x) \ dx}{\displaystyle\sum_{r=1}^{3} \int_r \rho_r \ \omega_j^2 \ \mathbf{\Phi}_j^T(x)\mathbf{\Phi}_j(x) \ dx} = \frac{\displaystyle\int_k \rho_k \mathbf{\Phi}_j^T(x)\mathbf{\Phi}_j(x) \ dx}{\displaystyle\sum_{r=1}^{3} \int_r \rho_r \mathbf{\Phi}_j^T(x)\mathbf{\Phi}_j(x) \ dx} \tag{33}$$

where ρ_k is the mass per unit length of the sub-structure and x is the generic space variable defined in the section II.

4. Modes classification

Modes of the studied structure are classified in four families depending on the relative importance of KER for each sub-structure. This classification is qualitative. Note that an arbitrary threshold on criterion KER could be defined to fix this classification in a quantitative manner.

- Modes 1, 3, 6, 11, 13 are beam modes: beam KER is one order higher than the string KER therefore the beam is the predominant sub-structure. If we compare beam modes (table II left column) to uncoupled beam modes (middle column), we notice that the beam-string coupling increases the beam mode's eigenfrequencies: each string acts as a stiffener [13]. Moreover, the first eigenfrequencies of an uncoupled beam constrained by no displacement at the positions of string supports (table II right column) have the same order of magnitude than those of the beam modes (left column). It indicates that strings approximatively behave as rigid supports. However, the discrepancies between the two sets of eigenfrequencies are all the more important as the frequency is high, and show the importance of the beam-string coupling.

- Modes 2, 7, 10, 12 are string modes: E_2 or E_3 string KER is one order higher than the two other KER therefore one string is the predominant sub-structure. In table II, string mode frequencies are slightly affected by the beam. This shows that the beam almost behaves like a fixed end for the strings.

- Modes 4, 5, 14 are string-string modes: both string KER are of the same order and one order higher than beam KER, therefore the two strings are at the same time the predominant sub-structures. Modes 4 and 5 almost correspond to the first mode of the E_3 string and the second mode of the E_2 string. The difference is the relative phase between strings: for mode 4, the two strings are in phase at their connection point on the beam, whereas they are out of phase for mode 5 (figure 7-A). This explains the small shift of frequency and the lower participation of the beam for mode 5. Mode 14 corresponds to the third mode of the E_3 string and the sixth mode of the E_2 string. The out of phase corresponding mode cannot be found because of the frequency limitation of our model.

- Mode 9 is a beam-string mode: both beam KER and E_3 string KER are much higher than E_2 string KER therefore beam and E_3 string are the predominant sub-structures. Note that in association with mode 10, this mode should be expected to be a coupled string-string mode, corresponding to the second mode of the E_3 string and the fourth mode of the E_2 string.

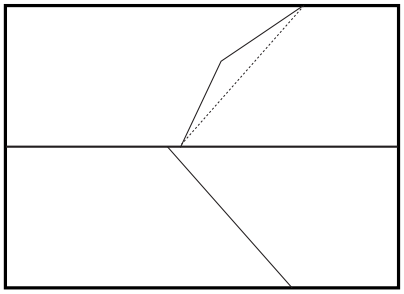

FIG. 6: E_3 string initial shape $w_s(x,0)$ obtained by plucking.

5. Definition of the sympathetic mode

We define the string-string mode as the *Sympathetic Mode* where strings KER have the same order of magnitude and are much higher than the beam KER. This qualitative definition of the sympathetic mode is consistent with the musician's definition of sympathetic vibrations: when one string is excited another string vibrates. Actually, according to the modal superposition principle [12], the response of the structure in the time domain can be obtained by summing the response of all modes,

$$\mathbf{q}(x,t) = \begin{pmatrix} u(x,t) \\ w(x,t) \end{pmatrix} = \sum_j a_j \mathbf{\Phi}_j(x) \cos(\omega_j t), \tag{34}$$

where t is the time and a_j is the modal amplitude depending on the initial condition

$$a_j = < \mathbf{q}(x,0), \mathbf{\Phi}_j > = \int_{\mathcal{S}} \rho_{\mathcal{S}} \begin{pmatrix} u(x,0) \\ w(x,0) \end{pmatrix}^T \mathbf{\Phi}_j dx. \tag{35}$$

The initial velocities equalling zero, terms on the form $\sin(\omega_j t)$ do not exist in (34) as they would be expected to, in the general case. The initial shape $w(x,0)$ of a string is given by figure 6 in the case of string plucking. If this shape is such that a_j does not equal zero, mode j is excited. If this mode is a sympathetic mode, both strings will be excited at the same time and the ratio of energy in each string is given by the KER.

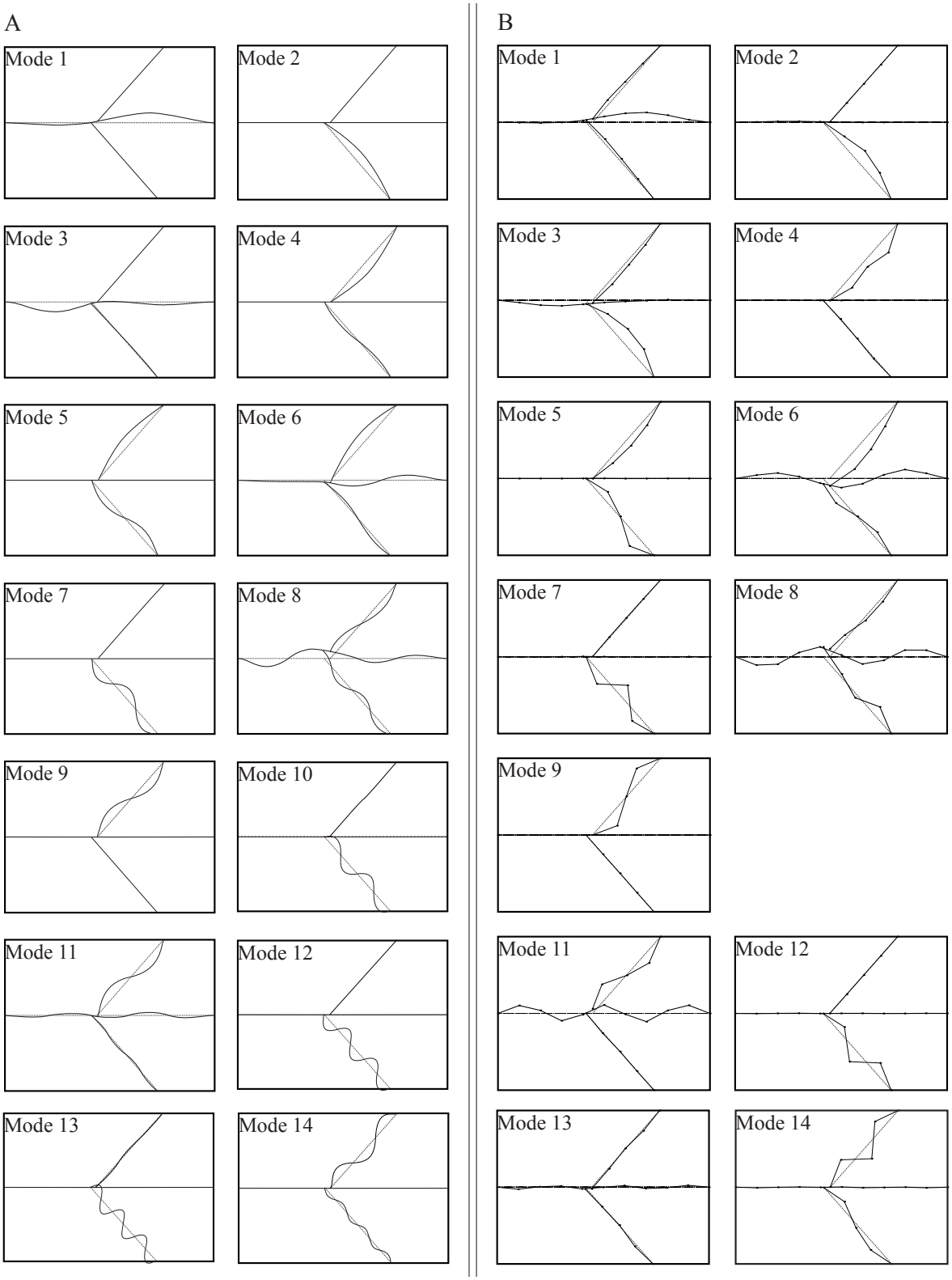

FIG. 7: A-Theoretical mode shapes obtained by transfer matrix method. Mode number is associated to eigenfrequency shown in table II.
B-Experimental mode shapes obtained by modal analysis on 11 measurement points on the beam and 3 on the string. Eigenfrequency of modes are shown in table III.

C. Experimental modal analysis

1. Description of the experimental setup

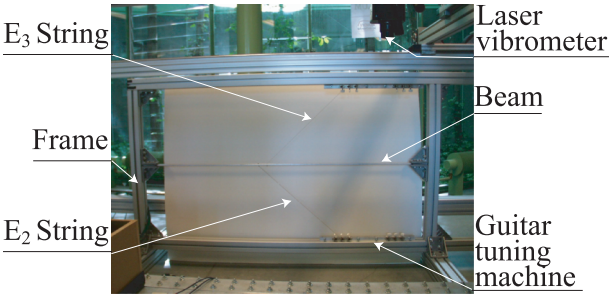

FIG. 8: Experimental setup showing the beam-2 strings assembly and the moving laser vibrometer.

The beam-2 strings assembly presented in figure 3 is studied by modal testing in order to confirm theoretical results.

The experimental setup is shown in figure 8. The beam is clamped onto a frame filled with sand to avoid interference with assembly modes. The steel strings are fixed, on one side, by a ring stuck in the beam, and on the other side, by a guitar tuning machine fixed on the frame. A guitar tuning machine is used to tune the strings at E_2 and E_3.

The experimental modal testing consists in measuring the frequency response functions between velocity and applied force at different points on the structure. From these data, we may extract eigenfrequencies, mode shapes and damping parameters of the studied structure using the Least Square Complex Exponential Method [14] as implemented in LMS software.

Because it is difficult to hit a string with a hammer, the hammer is used on one point of the beam to excite our system while a laser vibrometer measures the velocity response at all points: 11 on the beam and 3 on each string.

2. Results

In table III, the eigenfrequencies resulting from the modal analysis are presented in frequency range 0-550 Hz. In order to compare experimental eigenfrequencies with theoretical ones, we plot experimental against theoretical values, in figure 9. Each number of experimental mode corresponds to the number of the associated theoretical mode, obtained by studying mode shapes, (figure 7). Note that, in table III, a theoretical mode is missing, mode 10. We suggest that this problem is due to E_2 string measurements. In figure 9, we show that there is a good agreement between measured and theoretical modes: the average difference is about 8% with a maximum of about 25% for modes 3 and 8. However, a slight

Mode	Freq.	$\mathrm{KER}_j(k)$			Kind
j	(Hz)	k=0	k=1	k=2	of mode
1	52.01	100	0	0	**Beam**
2	82.70	21	79	0	**Beam-String**
3	86.31	88	12	0	**Beam-String**
6	135.30	98	1	1	**Beam**
4	165.10	6	1	93	**String**
5	167.00	0	85	14	**String-String**
8	218.45	99	1	0	**Beam**
7	250.16	3	97	0	**String**
11	314.42	99	0	1	**Beam**
9	330.24	0	0	100	**String**
12	418.04	1	99	0	**String**
13	442.09	99	1	0	**Beam**
14	496.10	14	35	50	**Beam-String-String**

TABLE III: Experimental eigenfrequencies, kinetic energy ratio and kinds of modes obtained by modal analysis for 2 strings connected to the beam.

frequency deviation exists for beam modes and this suggests that the ideal clamped end condition is not well satisfied in practice.

For each measured mode, the criterion KER, defined by equation (33), is also computed from the mode shape and then the kind of mode is determined. For the last modes, mode 12 to 14, the two strings KER are questionable because of few measurement points on strings, as shown in figure 9-B, and will not be discussed. Four kinds of mode are also obtained and particularly, string-string modes, although only one string-string mode has been extracted: mode 4.

The good agreement between experimental and theroretical results shows that the transfer matrix method is a valuable approach for the vibratory behaviour of the studied structure, and validates the proposed modes categorization.

D. Influence of inharmonicity on string-string mode

In order to investigate the sympathetic behaviour of the beam-2 strings model, we study the influence of the inharmonicy of the two strings on the KER criterion of string-string

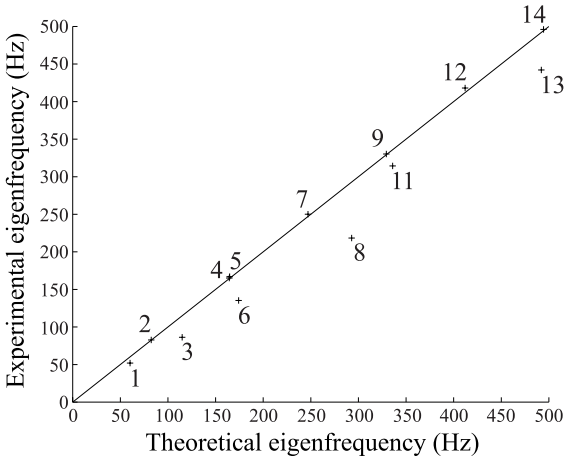

FIG. 9: Experimental eigenfrequencies as a function of theoretical eigenfrequencies. Mode number correspond to table II theoretical results and table III experimental results.

modes. Inharmonicity quantifies how out-of-tune the strings are and is defined by

$$\epsilon = \frac{f_2 - 2f_1}{2f_1}, \tag{36}$$

where f_1 and f_2 are the fundamental frequencies of the uncoupled E_2 and E_3 strings. For this study, we fix f_2 ($f_2 = 164.8$ Hz) and only f_1 is modified (from $f_1 = 80.4$ Hz to $f_1 = 84.4$ Hz). For a set of strings pair's frequencies, modes of the assembly are performed, by using the theoretical approach given section II, and kinetic energy ratio of each sub-structure for four modes are computed, see figure 10. Moreover we show the evolution of mode shapes for two inharmonicities: $\epsilon = -0.6\%$ and $\epsilon = 0.6\%$ which respectively correspond to $f_1 = 82.9$ Hz and $f_1 = 81.9$ Hz. These mode shapes allow us to link the kinetic energy ratio to its implications for string-string modes when inharmonicity differs from zero.

In figure 10, the case studied in section III can be seen when the two strings are tuned on octave, $\epsilon = 0$, and the kinetic energy ratios of the two strings do not equal: 25% and 69% for E_2 string and E_3 string respectively in the case of mode 4, 43% and 37% in the case of mode 10, 0% and 89% in the case of mode 9 and 97% and 0% in the case of mode 10. To obtain equal kinetic energy ratio for the two strings (close to 50%), the inharmonicity value is approximatively 0.25% which corresponds in musical scale at 4 cents. In order to have the two strings taking an equal part in the sympathetic mode, they must be 4 cents out-of-tune. Note that this value is obtained for curves which have the same aspect, modes 4, 9 and 10, but also for mode 5's curve which is more disrupted. Actually, for this mode there are three values in the case of equipartition of the strings's kinetic energy ratios as shown in figure 10.

For modes 4, 5, 9, 10, the strings's KER have the same evolution: while one of the strings's KER goes from 0% to 100% the other one goes from 100% to 0%. When the strings's KER switch, they have the same order of magnitude and thus the string-string

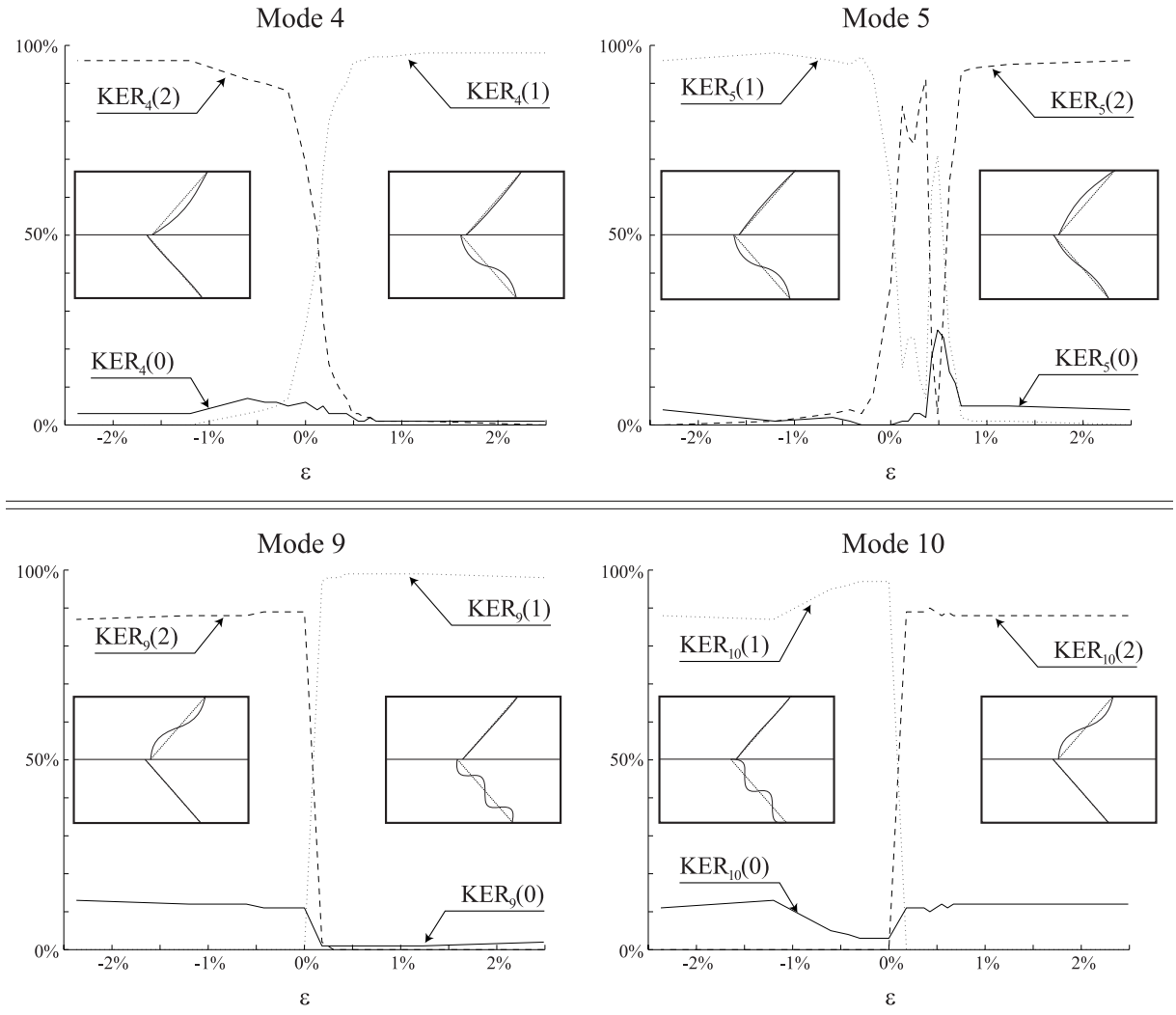

FIG. 10: kinetic energy ratio, $\mathrm{KER}_j(k)$ for each sub-structure k ($k = 0$ for the beam, $k = 1$ for the E_2 string and $k = 2$ for the E_3 strings) in relation to inharmonicity ($\epsilon = \frac{f_2 - 2f_1}{2f_1}$) on modes j 4, 5, 9 and 10. The two mode shapes corresponding to $\epsilon = -0.6\%$ ($f_1 = 82.9$ Hz) on the left and $\epsilon = 0.6\%$ ($f_1 = 81.9$ Hz) on the right of each curves are shown.

mode may appear. Inharmonicity range of the strings's KER switch is different for each mode: mode 4 and 5 ranges are larger than mode 9 and 10. This fact can explain why in the case studied in section III, $\epsilon = 0$, string-string modes are not obtained for mode 9 and 10, section III B 4, for the strings are not exactly 4 cents out-of-tune.

Note that the beam can play an important part in the string-string mode. Actually, for mode 5, the coupling with the beam is simultaneous with the strings's KER switch. Thus, at the switching moment it may be obtained not only sympathetic modes but also a beam-string mode.

IV. CONCLUSION

In order to consider the sympathetic phenomenon, an analytical model of a generic string instrument, composed of a beam-N strings assembly, has been studied by means of the transfer matrix approach, then the modal basis has been derived. A simplified system, a beam-2 strings assembly, has been extensively analysed. One string being tuned on octave away from the other (E2 and E3), several specific modes called "string-string modes" among three other kinds of modes, are extracted from the modal basis. The modes have been analysed and classified through the comparison of the kinetic energy ratio of each sub-structure (E_2 string, E_3 string and beam). String-string modes are responsible for the sympathetic phenomenon.

Furthermore, the modal basis of the beam-2 strings assembly has been extracted by measurements. A good agreement between eigenfrequencies and mode shapes is highlighted through theoretical results and experiments. Experimental results have been interpreted in terms of kind of modes previously given, and string-string modes have been observed. Moreover we have focussed our attention on the theoretical influence of string's inharmonicity on the string-string mode. On one hand, it is noticeable that the particular case of null inharmonicity between the two strings, does not correspond to the equipartition of the string's kinetic energy ratios. On the other hand, the inharmonicity range in which the string-string mode exists, when that the two string's kinetic energy ratios have the same order of magnitude, is narrow.

The model is one-dimensional and this fact is the main restriction for direct application to a real string instrument. Other limitations are related to the conservative hypothesis, that is retained for the normal mode computation. Moreother, torsional motions of the strings are not taken into account. The limitation of the method is the numerical difficulties of the transfer matrix method which occur at high frequencies.

The method and the results that we have presented are applicable to systems with many strings comparable to real string instruments, such as the harp. Harp players are annoyed by the acoustic consequence of the sympathetic phenomenon caused by the high number of strings. A question is, how can this annoyance be reduced? A way to investigate this problem is to do time domain simulations based on the modal basis of the string instrument, and to show the influence of string-string modes on the radiated sound, for instance. A parametric study of the different characteristics of the simplified instrument can be carried out to see their influence on string-string modes.

APPENDIX A: TRANSFER MATRIX OF A STRING'S SEGMENT

Each string is considered as perfectly flexible and stretched at tension T_0 made from a material whose Young's modulus is E_s and mass per unit length is ρ_s. The area of the cross section is denoted A_s. Strings are submitted to longitudinal and transverse displacements described by the equations of motion given by rod's theory and by string's theory [11]. These equations may be written in state form (3), in which the characteristic matrix, is given by

$$\mathrm{H}_s(\omega) = \begin{pmatrix} 0 & 0 & 1/E_sA_s & 0 \\ 0 & 0 & 0 & 1/T_0 \\ -\rho_s\omega^2 & 0 & 0 & 0 \\ 0 & -\rho_s\omega^2 & 0 & 0 \end{pmatrix}, \tag{A1}$$

and is associated to the state vector (1). Calculation of the eigenvalues of matrix $\mathrm{N}_s = -\jmath\mathrm{H}_s$ provides the wavenumbers of the longitudinal and transverse waves travelling in the strings: k_l, $-k_l$, k_t, $-k_t$, where

$$k_l = \omega\sqrt{\frac{\rho_s}{E_sA_s}} \quad \text{and} \quad k_t = \omega\sqrt{\frac{\rho_s}{T_0}}. \tag{A2}$$

Transfer matrix between points at coordinates x and x_0 is obtained from relation (5) as

$$T_s(x, x_0) = \begin{pmatrix} T_{s11}(x, x_0) & 0 & T_{s13}(x, x_0) & 0 \\ 0 & T_{s22}(x, x_0) & 0 & T_{s24}(x, x_0) \\ T_{s31}(x, x_0) & 0 & T_{s11}(x, x_0) & 0 \\ 0 & T_{s42}(x, x_0) & 0 & T_{s22}(x, x_0) \end{pmatrix}, \tag{A3}$$

where

$$\begin{aligned} T_{s11}(x, x_0) &= \cos(k_t(x - x_0)), & T_{s13}(x, x_0) &= \frac{k_t}{\rho_s\omega^2}\sin(k_t(x - x_0)), \\ T_{s22}(x, x_0) &= \cos(k_f(x - x_0)), & T_{s24}(x, x_0) &= \frac{k_f}{\rho_s\omega^2}\sin(k_f(x - x_0)), \\ T_{s31}(x, x_0) &= -\frac{\rho_s\omega^2}{k_t}\sin(k_t(x - x_0)), & T_{s42}(x, x_0) &= -\frac{\rho_s\omega^2}{k_f}\sin(k_f(x - x_0)). \end{aligned}$$

APPENDIX B: TRANSFER MATRIX OF A BEAM'S SEGMENT

The beam is supposed to be prismatic and made from material whose Young's modulus is E_b and mass per unit length is ρ_b. The area of the cross section is A_b and the second moment of area is I. Transverse and longitudinal motions of the beam are respectively described using Euler-Bernoulli theory and rod's theory [12]. Using state vector formalism, the equations of motion can be written on the form (3), in which the characteristic matrix

is given by

$$\mathrm{H}_b(\omega) = \begin{pmatrix} 0 & 0 & 0 & 1/E_bA_b & 0 & 0 \\ 0 & 0 & 1 & 0 & 0 & 0 \\ 0 & 0 & 0 & 0 & 0 & 1/E_bI \\ -\rho_b\omega^2 & 0 & 0 & 0 & 0 & 0 \\ 0 & -\rho_b\omega^2 & 0 & 0 & 0 & 0 \\ 0 & 0 & 0 & 0 & -1 & 0 \end{pmatrix}. \tag{B1}$$

Bending and longitudinal waves propagate with wavenumbers k_b, $-k_b$, $\jmath k_b$, $-\jmath k_b$, k_r, $-k_r$, where

$$k_b = \sqrt{\omega}\sqrt[4]{\frac{\rho_b}{E_bI}} \quad \text{and} \quad k_r = \omega\sqrt{\frac{\rho_b}{A_bE_b}}. \tag{B2}$$

These six values are the eigenvalues of matrix $\mathrm{N}_b = -\jmath\mathrm{H}_b$. Calculation of the associated eigenvectors gives the transfer matrix from relation (4). It is convenient to introduce the Duncan's functions [12], defined by the relations, in which ξ is a real parameter,

$$\begin{aligned} s_1(\xi) &= \sin(\xi) + \sinh(\xi) \\ c_1(\xi) &= \cos(\xi) + \cosh(\xi) \\ s_2(\xi) &= -\sin(\xi) + \sinh(\xi) \\ c_2(\xi) &= -\cos(\xi) + \cosh(\xi), \end{aligned} \tag{B3}$$

to express the transfer matrix,

$$T_b(x, x_0) = \begin{pmatrix} T_{b11}(x,x_0) & 0 & 0 & T_{b14}(x,x_0) & 0 & 0 \\ 0 & T_{b22}(x,x_0) & T_{b23}(x,x_0) & 0 & T_{b25}(x,x_0) & T_{b26}(x,x_0) \\ 0 & T_{b32}(x,x_0) & T_{b22}(x,x_0) & 0 & T_{b35}(x,x_0) & T_{b36}(x,x_0) \\ T_{b41}(x,x_0) & 0 & 0 & T_{b11}(x,x_0) & 0 & 0 \\ 0 & T_{b52}(x,x_0) & T_{b53}(x,x_0) & 0 & T_{b22}(x,x_0) & T_{b56}(x,x_0) \\ 0 & T_{b62}(x,x_0) & T_{b63}(x,x_0) & 0 & T_{b65}(x,x_0) & T_{b22}(x,x_0) \end{pmatrix}. \tag{B4}$$

After calculations, we find:

$$
\begin{aligned}
T_{b11}(x,x_0) &= \cos(k_t(x-x_0)), & T_{b14}(x,x_0) &= \frac{1}{k_t E_b A_b}\sin(k_t(x-x_0)),\\
T_{b22}(x,x_0) &= \frac{1}{2}c_1(k_f(x-x_0)), & T_{b23}(x,x_0) &= \frac{{k_f}^3 E_b I}{2\rho_b\omega^2}s_1(k_f(x-x_0)),\\
T_{b25}(x,x_0) &= -\frac{k_f}{2\rho_b\omega^2}s_2(k_f(x-x_0)), & T_{b26}(x,x_0) &= -\frac{k_f^2}{2\rho_b\omega^2}c_2(k_f(x-x_0)),\\
T_{b32}(x,x_0) &= \frac{\rho_b\omega^2}{2{k_f}^3 E_b I}s_2(k_f(x-x_0)), & T_{b35}(x,x_0) &= -\frac{1}{2k_f^2 E_b I}c_2(k_f(x-x_0)),\\
T_{b36}(x,x_0) &= \frac{1}{2k_f E_b I}s_1(k_f(x-x_0)), & T_{b41}(x,x_0) &= -A_b E_b k_t \sin(k_t(x-x_0)),\\
T_{b52}(x,x_0) &= -\frac{\rho_b\omega^2}{2k_f}s_1(k_f(x-x_0)), & T_{b53}(x,x_0) &= -\frac{k_f^2 E_b I}{2}c_2(k_f(x-x_0)),\\
T_{b56}(x,x_0) &= -\frac{k_f}{2}s_2(k_f(x-x_0)), & T_{b62}(x,x_0) &= \frac{\rho_b\omega^2}{2k_f^2}c_2(k_f(x-x_0)),\\
T_{b53}(x,x_0) &= \frac{k_f E_b I}{2}s_2(k_f(x-x_0)), & T_{b65}(x,x_0) &= -\frac{1}{2k_f}s_1(k_f(x-x_0)).
\end{aligned}
$$

APPENDIX C: DEMONSTRATION OF RELATION (19)

In this appendix we demonstrate the relation (19). This relation can be demonstrated in two steps. The first step is the demonstration of the recurrence relation, defined by, for $i = 1...N$,

$$\boldsymbol{\mathcal{X}_b}(O_i^+) = \mathrm{T}_b(O_i^-, A)\boldsymbol{\mathcal{X}_b}(A) + \sum_{j=1}^{i}\left[\mathrm{T}_b(O_i^-, O_j^+)\mathrm{K}_j\mathrm{T}_s(O_j, C_j)\boldsymbol{\mathcal{X}_s}(C_j)\right]. \tag{C1}$$

- We verify the relation (C1) for i=1. In that case (C1) is written as

$$\boldsymbol{\mathcal{X}_b}(O_1^+) = \mathrm{T}_b(O_1^-, A)\boldsymbol{\mathcal{X}_b}(A) + \mathrm{T}_b(O_1^-, O_1^+)\mathrm{K}_1\mathrm{T}_s(O_1, C_1)\boldsymbol{\mathcal{X}_s}(C_1). \tag{C2}$$

  As $\boldsymbol{\mathcal{X}_b}(O_1^-) = \mathrm{T}(O_1^-, A)\boldsymbol{\mathcal{X}_b}(A)$, $\mathrm{T}_b(O_1^-, O_1^+) = I_6$ and $\boldsymbol{\mathcal{X}_s}(O_1) = \mathrm{T}_s(O_1, C_1)\boldsymbol{\mathcal{X}_s}(C_1)$,

$$\boldsymbol{\mathcal{X}_b}(O_1^+) = \boldsymbol{\mathcal{X}_b}(O_1^-) + \mathrm{K}_1\boldsymbol{\mathcal{X}_s}(O_1) \tag{C3}$$

  in accordance with (17), the relation (C2) is true.

- We assum that the relation (C1) is valid for the i-string , we show that this relation C1) is still valid for the $i+1$-string . Let's consider the coupling relation (17) induced by the connection between the beam and the $i+1$-string,

$$\boldsymbol{\mathcal{X}_b}(O_{i+1}^+) = \boldsymbol{\mathcal{X}_b}(O_{i+1}^-) + \mathrm{K}_{i+1}\boldsymbol{\mathcal{X}_s}(O_{i+1}), \tag{C4}$$

  and taking the form of

$$\boldsymbol{\mathcal{X}_b}(O_{i+1}^+) = \mathrm{T}_b(O_{i+1}^+, O_i^+)\boldsymbol{\mathcal{X}_b}(O_i^+) + \mathrm{K}_{i+1}\mathrm{T}_s(O_{i+1}, C_{i+1})\boldsymbol{\mathcal{X}_s}(C_{i+1}). \tag{C5}$$

As we have the relation (C1), the relation (C2) is equivalent to

$$\boldsymbol{\mathcal{X}_b}(O_{i+1}^+) = \mathrm{T}_b(O_{i+1}^-, O_i^+)\mathrm{T}_b(O_i^-, A)\boldsymbol{\mathcal{X}_b}(A) + \sum_{j=1}^{i+1}\left(\mathrm{T}_b(O_{i+1}^-, O_j^+)\mathrm{K}_j\mathrm{T}_s(O_j, C_j)\boldsymbol{\mathcal{X}_s}(C_j)\right) \tag{C6}$$

since we have $\mathrm{T}_b(O_{i+1}^-, A) = \mathrm{T}_b(O_{i+1}^-, O_i^+)\mathrm{T}_b(O_i^-, A)$, relation (C6) gives

$$\boldsymbol{\mathcal{X}_b}(O_{i+1}^+) = \mathrm{T}_b(O_{i+1}^-, A)\boldsymbol{\mathcal{X}_b}(A) + \sum_{j=1}^{i+1}\left(\mathrm{T}_b(O_{i+1}^-, O_j^+)\mathrm{K}_j\mathrm{T}_s(O_j, C_j)\boldsymbol{\mathcal{X}_s}(C_j)\right) \tag{C7}$$

Relation (C7) proves that (C1) is valid for i+1 string.

- Finally, we prove the relation (C1), for $i = 1...N$:

$$\boldsymbol{\mathcal{X}_b}(O_i^+) = \mathrm{T}_b(O_i^-, A)\boldsymbol{\mathcal{X}_b}(A) + \sum_{j=1}^{i}\left[\mathrm{T}_b(O_i^-, O_j^+)\mathrm{K}_j\mathrm{T}_s(O_j, C_j)\boldsymbol{\mathcal{X}_s}(C_j)\right]. \tag{C8}$$

The second step is the insersion in the coupling relation (18) of the recurrence relation (C1). These two relations, (18) and (C1), along with the transfer relation between state vectors $\boldsymbol{\mathcal{X}_s}(O_i)$ and $\boldsymbol{\mathcal{X}_s}(C_i)$, given by

$$\boldsymbol{\mathcal{X}_s}(O_i) = \mathrm{T}(x_{O_i}, x_{C_i})\boldsymbol{\mathcal{X}_b}(C_i), \tag{C9}$$

leads us to obtain the relation (19).

Acknowledgments

The authors acknowledge financial support from the CNRS and the Region des Pays de la Loire for JLLC's PhD studentship. They also acknowledge the students of ENSIM: R. Arnaud, O. Doutres and S. Paillasseur for setting up the experiment and for the first computerized model.

[1] L.C. Morfey. *Dictionary of acoustics*. Academic Press, 2001.

[2] L. Greilsamer. *Le baryton du prince esterhazy*. Librairie La flute de Pan, 1981.

[3] C.M. Hutchins. Sympathetic vibration and coupling of resonances. *J. Catgut Acoust. Soc.*, 1:40–41, 1990.

[4] C.E. Gough. The theory of string resonances on musical instruments. *Acustica*, 49:124–141, 1981.

[5] G. Weinreich. Coupled piano strings. *J. Acoust. Soc. Am.*, 62(6):1474–1484, 1977.

[6] B. Capleton. False beats in coupled piano string unisons. *J. Acoust. Soc. Am.*, 115(2):885–892, 2004.

[7] V. Valimaki M. Karjalainen and Z. Janosy. Towards high-quality sound synthesis of the guitar and string instruments. *Proceedings of the 1993 International Computer Music Conference*, 1993.

[8] E.C. Pestel and F.A. Leckie. *Matrix method in elastomechanics.* McGraw-Hill, 1963.

[9] Z. Wang and A.N. Norris. Waves in cylindrical shells with circumferential submembers: a matrix approach. *J. Sound Vib.*, 181:457–484, 1995.

[10] M-H. Moulet. *Les jonctions en mécanique vibratoire: représentation par matrice de diffusion et caractérisation expérimentale pour des poutres assemblées.* PhD thesis, Université du Maine, 2003.

[11] C. Valette and C. Cuesta. *Mécanique de la corde vibrante.* Hermes, 1993.

[12] M. Géradin and D. Rixen. *Théorie des vibrations, application à la dynamique des structures.* Masson, 1996.

[13] Z. Oniszczuk. Free transverse vibrations of an elastically connected complex beam-string system. *J. Sound Vib.*, 254(4):703–725, 2002.

[14] D.J. Ewins. *Modal testing: theory and practice.* John Wiley and Sons, 1994.